

PAPER • OPEN ACCESS

## Evaluation of Vulcanization Depth of Thick Rubber Products by Terahertz Radiation

To cite this article: Y Yasumoto *et al* 2019 *IOP Conf. Ser.: Mater. Sci. Eng.* **548** 012003

View the [article online](#) for updates and enhancements.

# Evaluation of Vulcanization Depth of Thick Rubber Products by Terahertz Radiation

Y Yasumoto<sup>1</sup>, Y Hirakawa<sup>1</sup>, and T Gondo<sup>1</sup>

<sup>1</sup>. National Institute of Technology, Kurume College, 1-1-1 Komorino, Kurume 830-8555, Japan

E-mail: hirakawa@kurume-nct.ac.jp

**Abstract.** An evaluation of the vulcanization depth of thick rubber products was performed using terahertz (THz) time-domain spectroscopy. The sample herein was a styrene-butadiene rubber (SBR)-based cylindrical products with a 35 mm diameter and 20 mm thickness, vulcanized under 10 MPa of pressure and a temperature of 150 °C. To clarify the vulcanization effect, no carbon black (CB) was included in the sample, because its apparent THz absorbance is extremely large compared with that of polymers and other additives. To perform the THz absorbance imaging, the thick sample was sliced parallel to the upper and lower heating plates of the cure mold into six thin specimens a few millimeters thick. Herein, the samples cured for two different cure times ( $T_{90}$  and  $T_{100}$ ) were investigated and compared. It was found that the coefficient of variation (CV) of the THz absorbance in the sliced specimens was suitable for evaluating the cure condition in the thick sample. The THz imaging results were used to compare the crosslinking densities of the sliced specimens using the Flory-Rehner equation.

## 1. Introduction

THz radiation has both light-like and radio wave-like characteristics, because it lies between the microwave and infrared regions of the electromagnetic band, as shown in Fig. 1. It can penetrate most materials except metal and can be manipulated by mirrors and lenses [1]. There has been an attempt to use THz light for various industrial inspections such as paint films [2] and tablet coatings [3]. Further, THz radiation is suitable for nondestructive evaluation/inspection of materials including industrial products such as polymers and elastomers. Our research group has developed a novel technique using THz technology to evaluate rubbers, and various applications have been reported [4-7], and the THz imaging of a carbon black dispersion over an area several millimeters square and the possibility of visualizing the cure process have been described.

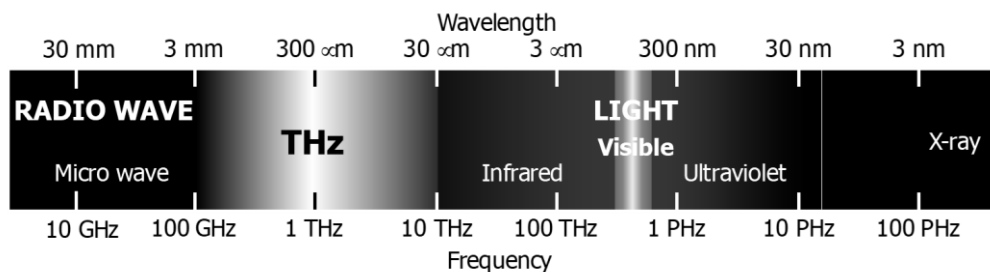


**Fig. 1.** THz region in the electromagnetic band

In this article, we report the estimation of the vulcanization depth of thick rubber products. The sample used was cylindrical with a thickness of 20 mm. This thick sample was sliced into several thin specimens each with a thickness of a few millimeters, and each specimen was evaluated by THz time-domain spectroscopy (THz-TDS) to obtain the THz absorbance images. It

**Table 1.** Compound formulation. The materials include styrene-butadiene rubber (SBR), tetramethylthiuram disulfide (TMTD), dibenzothiazole disulfide (MBTS) and n-cyclohexyl-2-benzothiazole sulfenamide (CBS).

Ingredient	Material	Quantity [phr]
Polymer	SBR	100
Accelerator/activators	Zinc oxide	5
	Stearic acid	1
Vulcanizing agent	Sulfer	1
Vulcanization accelerators	TMTD, MBTS, CBS	1 each

was found that the coefficient of variation (CV) of the THz absorbance dispersion is suitable for evaluating the degree of vulcanization at each depth position. The correlation between the THz absorbance values and the crosslinking density calculated using the Flory-Rehner equation [8] was confirmed using the same samples after soaked in toluene and swollen, indicating the validity of the THz evaluation proposed herein.

## 2. Experiment

### 2.1 Samples

The used samples used herein were vulcanized rubber based on styrene-butadiene rubber (SBR, the commercial grade: JSR 1502, JSR Co.), whose compounding formulation is given in Table 1. All the reagents used were commercial grade and supplied by Sanshin Chemical Industry Co., Ltd. To clarify the cure effect, no carbon black (CB) was included in the sample, because the apparent THz absorbance of CB is extremely large compared with polymers and other additives [4]. The samples were cured under 10 MPa of pressure and a temperature of 150 °C using a special mold for thick rubber production. The cure time  $T_{90}$  ( $T_{100}$ ) is defined as the time required for the torque to reach 90% (100%) of difference between the minimum and the maximum vulcanization curve torque.  $T_{90}$  is so-called optimum cure time. Herein,  $T_{90}$  and  $T_{100}$  for the thick samples were estimated using the results obtained by a thin ( $t = 2$  mm) sample having the same composition using a curemeter (JSR Trading Co., Ltd., Curelometer W). The cured thick sample was cylindrical with a 35 mm diameter and a thickness of 20 mm, which was sliced parallel to the upper and lower heating plates of the cure mold into six thin specimens with the thickness of about 3 mm thick, as shown in Fig. 2.

### 2.2 Experimental setup and method

To evaluate the rubber samples in this study, the spectroscopic technique of THz-TDS [9,10] was used, which is a unique and representative technique using THz radiation that characterizes material information such as transmission, absorption, reflection, and complex physical quantities

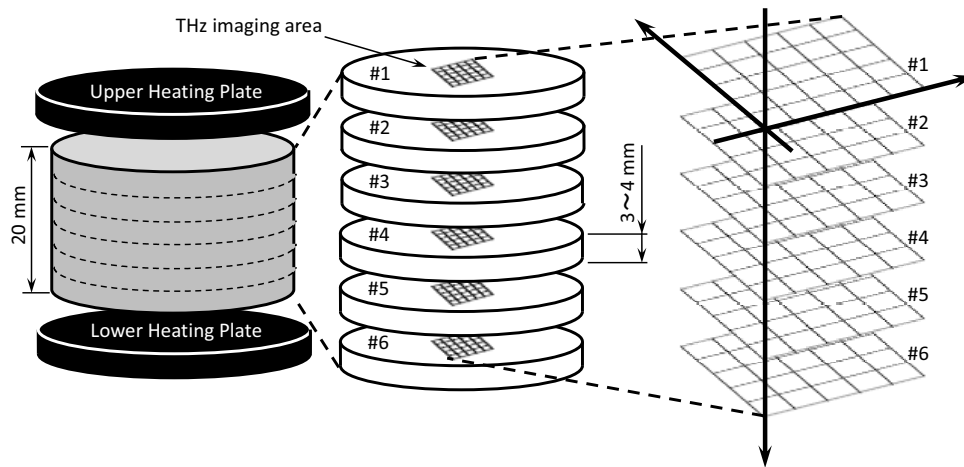


**Fig. 2.** Schematic of the thick sample used in this study (left), the six thin slices obtained from the thick samples (center), and the areas on each sample scanned by THz time-domain

by data processing. Figure 3 shows a schematic drawing of the THz-TDS system (Otsuka Electronics Co., Ltd., TR-100KS) used herein, in which a femtosecond fiber laser (IMRA America, Inc., Femtolite HX-150, 1620 nm, 100 fs) is used as the fundamental laser light source. In this study, the THz transmission was measured to obtain the THz absorbance. Herein, the THz radiation generated by the 4'-dimethylamino-N-methyl-4-stilbazolium tosylate (DAST) crystal was focused into the sample by the off-axis paraboloidal mirrors. The THz light that passed through the sample was detected by the photoconductive (PC) switch made of low-temperature-grown GaAs to record a real-time wave form  $E(t)$  in the computer. By converting the waveform by Fourier transformation, the frequency spectrum  $E(\omega)$  was derived as

$$E(\omega) = \int_{-\infty}^{\infty} E(t)e^{i\omega t} dt = |E(\omega)|e^{i\phi(\omega)},$$

where  $\omega$  and  $\phi$  are the angular frequency and the phase of the THz radiation, respectively. The frequency spectra for the reference (i.e., blank) and the sample were then calculated to obtain the absorbance  $A(\omega)$ , such that

$$A(\omega) = -\log \left| \frac{E_{sample}(\omega)}{E_{ref}(\omega)} \right|,$$

where the subscripts *sample* and *ref* indicate the sample and the reference spectra, respectively.

Because the absorbance is a function of the sample thickness, the THz absorbance obtained herein was converted into the value per unit thickness (1 cm). During the two-dimensional THz absorbance imaging measurement, the sample was raster scanned in the  $x$  – and  $y$  – axes on the sample stage in the THz-TDS system. The scanned area was 5 mm  $\times$  5 mm with an interval of 1 mm (25 sampling points) at the central part of each specimen, as depicted in Fig.2. The THz absorbance image was then constructed by calculating the representative THz absorption  $A_{image}(x,y)$  at each measured point  $(x,y)$ , which was calculated by integrating the THz absorbance spectrum as

$$A_{image}(x, y) = \int_{\omega_1}^{\omega_2} A_{x,y}(\omega) d\omega / (\omega_2 - \omega_1),$$

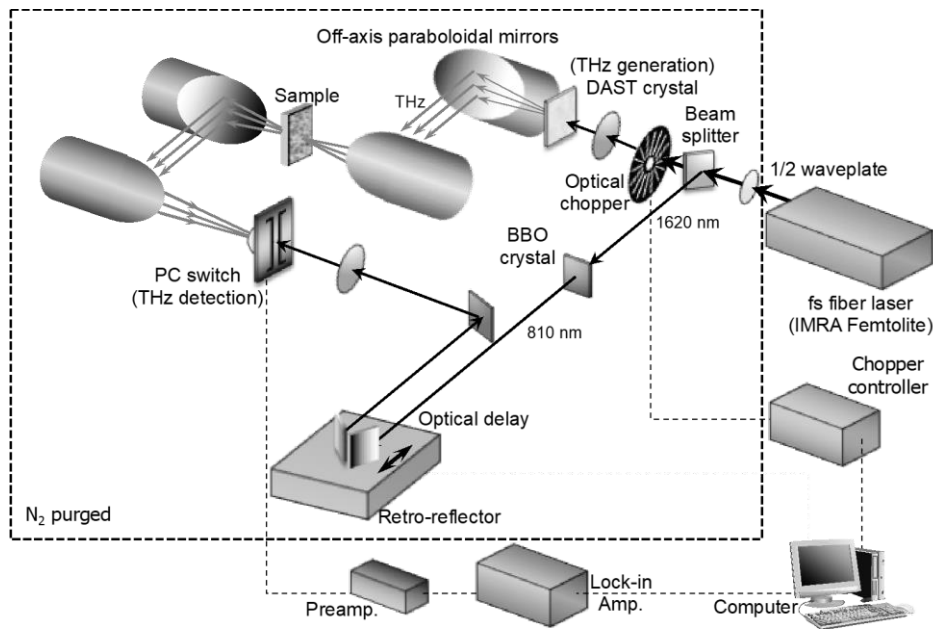


**Fig. 3.** Schematic of the THz time-domain spectroscopy system used in this study.

where  $\omega_1$  and  $\omega_2$  are the low- and high-end frequencies of the THz absorbance spectrum, respectively. The values for  $\omega_1$  and  $\omega_2$  were determined by the spectral region exhibiting a superior signal-to-noise ratio. In this study, the values of  $\omega_1$  and  $\omega_2$  were 0.21 and 2.7 THz, respectively.

To obtain the crosslinking densities, the used silenced samples were swelled in toluene at room temperature for 72 hours. After that, the samples were dried for 24 hours at 80 °C to vaporize toluene inside the samples. The crosslinking density of the sliced specimens were calculated by the Flory-Rehner equation,

$$v = \frac{V_R + \ln(1 - V_R) + \mu V_R^2}{-V \left( V_R^{\frac{1}{3}} - \frac{V_R}{2} \right)}$$

where  $V_R$  is the volume fraction of the polymer (i.e., SBR) in the swollen gel,  $V$  is the molar volume of the solvent (i.e., toluene), and  $\mu$  is the Flory solvent-polymer interaction term. The obtained densities were compared with the THz results to confirm the validity of the THz evaluations.

### 3. Results and discussion

According to our previous experimental results [7] after the optimum cure time  $T_{90}$ , the THz transmission becomes smaller as the vulcanization reaction progressed; namely, the THz absorbance of the rubbers increased with the cure process. However, the dispersion of the THz absorbance tends to gradually decrease with the cure time. Prior to imaging the slice specimens, this trend of the THz absorbance was confirmed using a thin (about 2 mm) SBR sample with the same compounding formulation shown in Table 1. In these experiments, a total of  $3 \times 3 = 9$  points

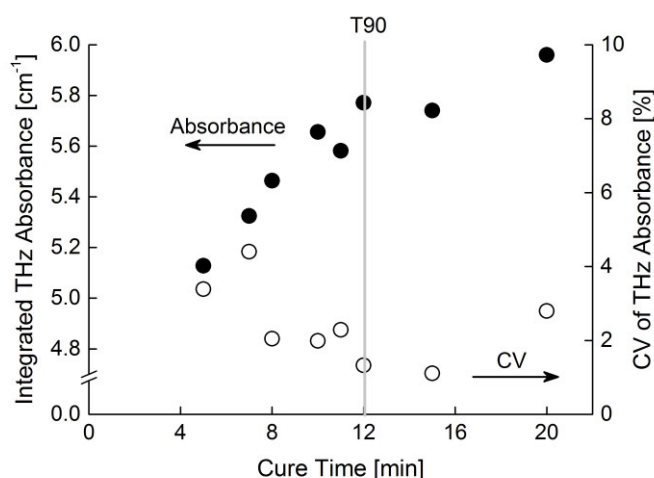


**Fig. 4.** Integrated THz absorbance (solid circles) and CV (open circles) of the THz absorbance dispersion of nine measured points in the thin sample. The line labeled T90 indicates the optimum cure time for the thin sample.

were evaluated by the THz-TDS system with a resolution of 1 mm. The result is summarized in Fig. 4, where the averaged THz absorbance and the coefficient of variation (CV) of the THz absorbance at the nine measured points are plotted against the cure time. The CV is a parameter indicating the rubber homogeneity. The optimum cure time of this thin sample was found to be 12 min, as indicated by the vertical line labeled T90 in Fig. 4. We found a prevailing tendency of the THz absorbance to gradually increase and of the CV to decrease with the cure time. These same parameter tendencies have been previously reported in Ref 7. This result suggests that, as the reaction proceeds, the THz radiation encounters increased disturbance in the sample such as absorption, scattering, and interference owing to unidentified chemical products or chemical structures (i.e., crosslinking) induced by the vulcanization, and the disturbances ultimately become homogeneous. Interestingly, we can observe the CV parameter to suddenly increase at 20 min (i.e., T100), which likely caused by polymers being cut or crosslinked by overcuring, indicating chaotic condition in the thin sample. It is well known that the crosslink density in rubber is formed by the vulcanization reaction [11], but the chemical condition of the crosslinking has not been fully revealed yet [12]. In a previous study we confirmed that the crosslink density in samples increased with the cure time and we have also found that the density curve of these samples exhibited a profile identical to the torque-cure curve obtained by a cure meter [7]. Based on these facts, it is reasonable to conclude that the observed increase of THz absorbance with the cure time can be correlated to the crosslink density in the sample, though an accurate accounting of the factors inducing the THz absorbance increase is still unclear. The possible candidates mentioned above can be considered as factors, but further detailed investigations are necessary to reveal this point.

The results of Fig. 4 confirm that the THz absorbance has a correlation with the crosslink density induced by the vulcanization reaction. As a next step, we conducted the THz imaging of the thick samples (i.e., sliced specimens shown in Fig. 2). The THz absorbance images of the thick samples at T90 and T100 are given in Fig. 5, where the dark and light contrast in the images show high and low THz absorbance, respectively. Comparing the images of the T90 and T100 samples, we can see that the latter sample exhibits darker image contrast than that of the former. This result shows that the vulcanization reaction in the sample at T100 may proceed farther than at T90, according to the result of Fig. 4. To recognize the difference between two samples clearly, the

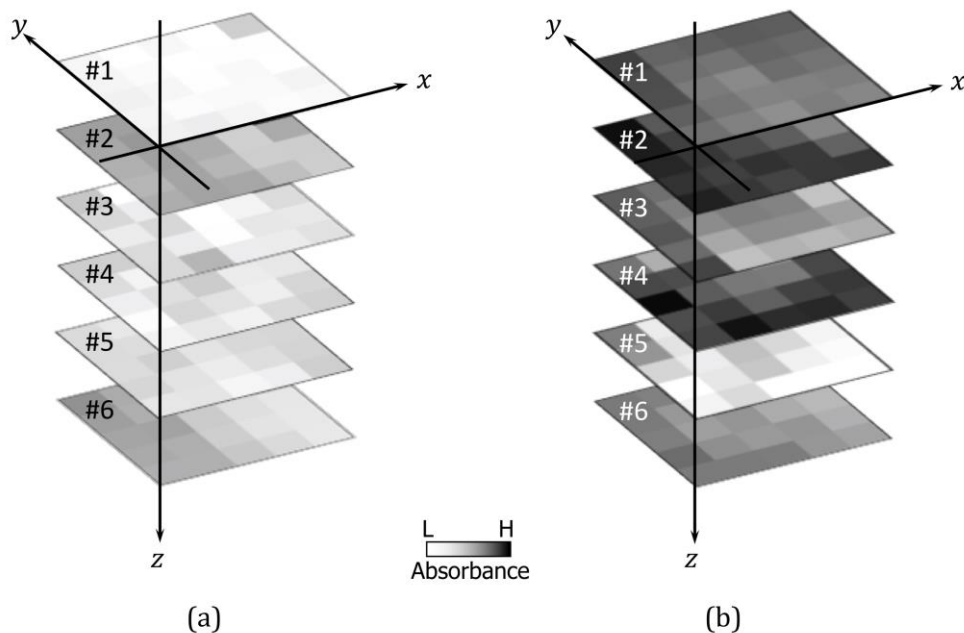


**Fig. 5.** Images mapping the THz absorbance for the (a) *T90* sample (b) *T100* sample.

average of the THz absorbance and the CV of the THz absorbance dispersion in one slice specimens were 2.27 and 2.29  $\text{cm}^{-1}$  for *T90* and *T100* sample, respectively, and the mean CVs of *T90* and *T100* samples were 2.59 and 2.54 %, respectively. These results suggest that the vulcanization process in the *T100* thick sample progressed farther and the reaction became more homogeneous than that of the *T90* sample. We also note the behavior of the CV values as a function of slice position in each sample, shown in Fig. 5, where the slice specimens are placed in sequence of height in the sample from the left to the right (the slice number is omitted). It can be seen that the CV values maximum at the center of the sample (slice #3 or #4), which indicates that the cure reaction is still active at the center slice specimen of each sample. It is reasonable to believe that an increased CV values reflects a random vulcanization condition (i.e., active condition), while a lower CV value is owing to a uniform reaction (i.e., calm condition). For example, at one point in the central specimen of the thick sample the reaction just started, and at other point in the same slice the reaction has almost finished. In the sliced specimens nearer the heating plates of the cure mold (especially #1 and #6 slices), the reactions have almost finished and the condition became rather homogeneous. Comparing the maximum CV value in each thick sample, the *T90* sample presents a larger CV peak than the *T100* sample, which is likely owing to the same theory posited above wherein the vulcanization reaction in the *T90* sample was more active than that of the *T100* sample. From these experimental results and our theory, we conclude that the CV of the THz absorbance dispersion is a suitable parameter for evaluating the degree of vulcanization at each depth position.

To confirm the validation of the cure condition as estimated by the THz absorbance and its dispersion, the conventional crosslink density of the samples was calculated based on the Flory-Rehner equation using the weights and volumes of the exact samples used in the THz evaluation (Fig. 5) and the solvent used in the equilibrium swelling experiment. In this study, toluene was selected as solvent. The obtained the crosslink densities for the *T90* and *T100* samples are plotted in Fig. 7, where the crosslink density in each sample slice (#1–#6) of the *T90* and *T100* samples

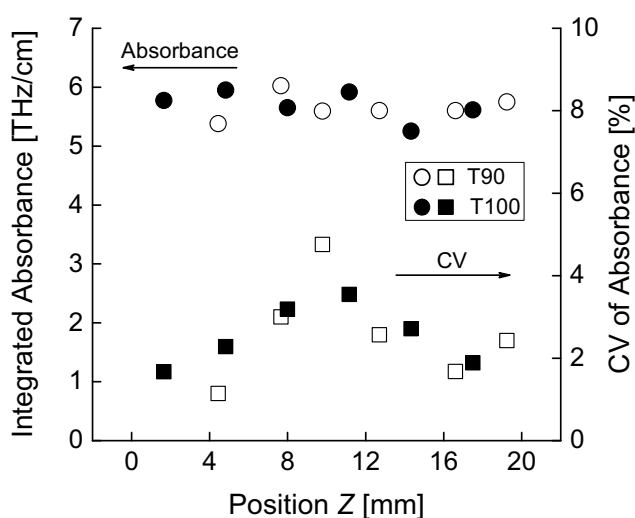


**Fig. 6.** Averages of the THz absorbance (circles) and CV (squares) of the absorbance dispersion in each slice.

are compared. The average densities were 0.192 and 0.221 mol/L for the *T90* and *T100* samples, respectively. As can be seen, the *T100* sample had more crosslink density, indicating that more revolution of the vulcanization reaction occurred. We also note that the clear trend of increased crosslink in the samples is confirmed by both the equilibrium swelling experiment and the THz absorbance imaging, as shown in Fig. 5 and Fig. 7.

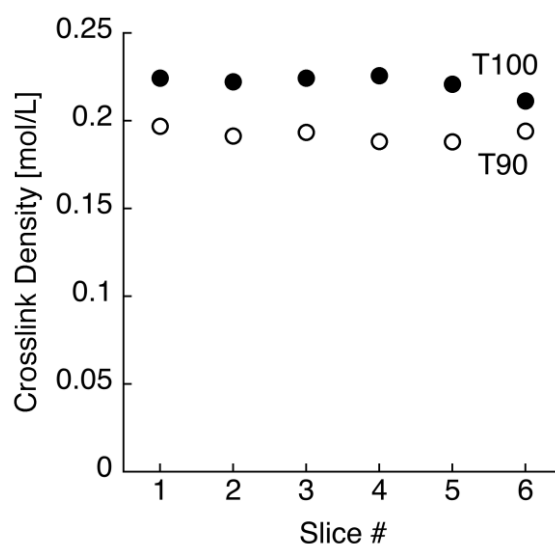


**Fig. 7.** Crosslink densities for the *T90* (open circles) and *T100* (solid circles) samples, as calculated by the Flory-Rehner equation.

Although the results obtained by the conventional swelling method is more obvious than that obtained by the THz experiment, the CV values of the THz absorbance also provide us information regarding the cure condition. Moreover, the THz absorbance measurements were obtained after only several hours via a nondestructive evaluation. The conventional equilibrium swelling method, however, required at least one week to obtain the final results and the samples were

completely destroyed. This comparison between these two-different evaluation methods indicates that our novel method using the THz absorbance for the vulcanization reaction is sufficiently effective. Further, the experimental results in this study suggest that the THz spectroscopic method has the potential to rapidly evaluate cure reactions in thick samples with no damage. We expect that the THz technique will successfully reveal unknown aspects of various elastomer products in the near future.

#### 4. Conclusion

An estimation of vulcanization depth of thick rubber products was performed using the THz-TDS technique. The thick sample (20 mm) was sliced parallel to the upper and lower heating plates of the cure mold into six thin specimens with a thickness of a few millimeters. Each specimen was evaluated at 25 different points to obtain the THz absorbance for the THz absorbance imaging. It was found that the THz absorbance values for each slice were almost constant, while the CV of the THz absorbance, which corresponds to the THz dispersion, had maximum value at the central slice of the thick sample. This behavior of the CV value suggests an active condition of the cure process at the center of the thick sample. We concluded that the CV parameter is suitable for evaluating the degree of vulcanization at each depth position in the sample. This study proved the effectiveness of non-destructive rapid THz estimation of the vulcanization as a function of depth in thick rubber products.

#### Acknowledgements

The authors thank Prof. M. Tonouchi of Osaka University, Japan, for his support on the THz systems, and Dr. H. Ohtake of IMRA America for his technical support. We thank Sara Maccagnano-Zacher, PhD, from Edanz Group ([www.edanzediting.com/ac](http://www.edanzediting.com/ac)) for editing a draft of this manuscript. This study was partially supported by the 23rd and 28th Eno Foundation for the Advancement of Science and the Japan Society for the Promotion of Science (JSPS) KAKENHI (Grant Nos 24560056 and 16K05925).

#### References

- [1] Tonouchi M 2007 *Nature Photonics* **1** 97
- [2] Yasui T, Yasuda T, Sawanaka K, Araki T 2005 *App. Opt.* **44** 6849
- [3] Fitzgerald AJ, Cole BE, Taday PF 2005 *J. Pharm. Sci.* **94** 177
- [4] Hirakawa Y, Ohno Y, Gondoh T, Mori T, Takeya K, Tonouchi M, Ohtake H, and Hirosumi T 2011 *J. Infrared, Millimeter and Terahertz Waves* **32** 1457
- [5] Hirakawa Y, Kamino T, Gondoh T, Hirano S, and Noguchi T 2016, *Proceeding of EMN Meeting on Terahertz 2016* (San Sebastián) C29
- [6] Hirakawa Y, Yamauchi T, Kamino T, Gondoh T, Hirano S, and Noguchi T 2017 *Technical Digests of the Conference on Lasers and Electro-Optics (CLEO) Optical Society of America* (San Jose), AT4B
- [7] Hirakawa Y, Nobutsuka A, Gondoh T, and Mori T 2015 *Proceedings of International Symposium on Frontiers in THz Technology (FTT 2015)* (Hamamatsu) Pos2.33
- [8] Flory P J, Rehner J 1943 *J. Chem. Phys.* **11** 521
- [9] Nishizawa S 2005 *Terahertz Time-Domain Spectroscopy* (Terahertz Optoelectronics) ed K Sakai (Heidelberg: Springer-Verlag) pp. 203-269
- [10] Baxter J B, Schmuttenmaer 2007 *Time-Resolved Terahertz Spectroscopy and Terahertz Emission Spectroscopy* (Terahertz Spectroscopy) ed SL Dexheimer (Boca Raton: CRC Press) chapter 3 pp. 73-118
- [11] Cpran A Y 2013 *Vulcanization* (The Science and Technology of Rubber, 4th edn) ed JE Mark, and B Erman and M Roland (Oxford: Academic Press) chapter 7 pp. 337-381
- [12] Sakai Y, Usami R, Tohsan A, Junkong P, Ikeda Y 2018 *RSC Adv.* **8** 10727